

# The Proper Motion of Sgr A\*: I. First VLBA Results

M. J. Reid

Harvard-Smithsonian Center for Astrophysics, Cambridge, MA 02138

A. C. S. Readhead & R. C. Vermeulen

California Institute of Technology, Pasadena, CA 91109

R. N. Treuhaft

Jet Propulsion Laboratory, Pasadena, CA 91109

## ABSTRACT

We observed Sgr A\* and two extragalactic radio sources nearby in angle with the VLBA over a period of two years and measured relative positions with an accuracy approaching 0.1 mas. The apparent proper motion of Sgr A\* relative to J1745–283 is  $5.90 \pm 0.4$  mas  $y^{-1}$ , almost entirely in the plane of the Galaxy. The effects of the orbit of the Sun around the Galactic Center can account for this motion, and any residual proper motion of Sgr A\*, with respect to extragalactic sources, is less than about  $20$  km  $s^{-1}$ . Assuming that Sgr A\* is at rest at the center of the Galaxy, we estimate that the circular rotation speed in the Galaxy at the position of the Sun,  $\Theta_0$ , is  $219 \pm 20$  km  $s^{-1}$ , scaled by  $R_0/8.0$  kpc.

Current observations are consistent with Sgr A\* containing all of the nearly  $2.6 \times 10^6 M_\odot$ , deduced from stellar proper motions, in the form of a massive black hole. While the low luminosity of Sgr A\*, for example, might possibly have come from a contact binary containing of order  $10 M_\odot$ , the lack of substantial motion rules out a “stellar” origin for Sgr A\*. The very slow speed of Sgr A\* yields a lower limit to the mass of Sgr A\* of about  $1,000 M_\odot$ . Even for this mass, Sgr A\* appears to be radiating at less than 0.1% of its Eddington limit.

*Subject headings:* Individual Sources: Sgr A\*; Black Holes; Galaxy: Center, Fundamental Parameters, Structure; Astrometry

## 1. Introduction

Sgr A\* is a compact radio source, similar to weak active nuclei found in other galaxies. Since its discovery more than two decades ago by Balick & Brown (1974), the possibility that Sgr A\* is a super-massive ( $\sim 10^6 M_\odot$ ) black hole has been actively considered. However, its radio luminosity of  $\approx 10^2 L_\odot$  (Serabyn et al. 1997) and its estimated total luminosity of  $\lesssim 10^5 L_\odot$  are many orders of magnitude below that possible from a  $\sim 10^6 M_\odot$  black hole. Thus, on the basis of its spectral energy distribution Sgr A\* could be an unusual contact binary containing  $\sim 10 M_\odot$  and radiating near its Eddington limit.

Recently, Eckart & Genzel (1997) and Ghez et al. (1999) measured proper motions of stars near the position of Sgr A\*, as determined by Menten et al. (1997). Stellar speeds in excess of 1000 km  $s^{-1}$  at a distance of 0.015 pc from Sgr A\* indicate a central mass of  $2.6 \times 10^6 M_\odot$ . While these dramatic results are consistent with the theory that Sgr A\* is a super-massive black hole, it is still conceivable that most of the central mass could come from a combination of stars and perhaps some form of dark matter. Clearly,

independent constraints on the mass of Sgr A\* are needed to establish whether or not it is a super-massive black hole nearly at rest at the dynamical center of the Galaxy.

The *apparent* motion of Sgr A\* can be used to estimate the mass and elucidate the nature of this unusual source. An apparent motion of Sgr A\* can be attributed to at least three possible components: 1) a secular motion induced by the orbit of the Sun about the Galactic Center, 2) a yearly oscillation owing to the Earth's orbital motion around the Sun (trigonometric parallax), and 3) a possible motion of Sgr A\* with respect to the dynamical center of the Galaxy. Measurement of, or limits for, these components of Sgr A\*'s apparent motion can provide unique information on the circular rotation speed ( $\Theta_0$ ) of the Local Standard of Rest (LSR) and the peculiar motion of the Sun ( $V_\odot$ ), the distance to the center of the Galaxy ( $R_0$ ), and the nature of Sgr A\* itself.

In 1991 we started a program with the Very Long Baseline Array (VLBA) of the National Radio Astronomy Observatory <sup>1</sup> (NRAO) to measure the apparent motion of Sgr A\*. In principle, VLBA observations of Sgr A\*, phase-referenced to extragalactic radio sources, can achieve an accuracy sufficient to detect secular motions of  $\lesssim 1 \text{ km s}^{-1}$  for a source at the distance of the Galactic Center. However, achieving this accuracy is quite challenging technically as it involves observing at short wavelengths (7 mm), in order to minimize the effects of interstellar scattering toward Sgr A\*, phase-referencing to extragalactic sources, and careful modeling of atmospheric effects (because of the low source elevations).

In the early years of the project, we searched for strong, compact, extragalactic sources nearby in angle to Sgr A\* and worked toward an optimum observing strategy. In this paper, we report results of observations spanning a two year period from 1995 to 1997. Our VLBA images clearly show movement of Sgr A\* with respect to extragalactic sources over many synthesized beams. While the current positional accuracy is inadequate to determine a trigonometric parallax, the secular motion of Sgr A\* is easily measured. This yields an accurate estimate of the angular rotation rate of the Sun around the Galactic Center,  $(\Theta_0 + V_\odot)/R_0$ , and places interesting limits on the mass of the black hole candidate responsible for the radio emission. Our results, and those of Backer and Sramek (1999) from observations with the Very Large Array (VLA) over a 15 year period, indicate that the apparent proper motion of Sgr A\* is dominated by the orbit of the Sun about the Galactic Center and that any peculiar motion of Sgr A\* is very small.

## 2. Observations

Our successful observations using the VLBA were conducted in the late-night, early-morning periods of 1995 March 4, 1996 March 20 and 31, and 1997 March 16 and 27. (Observations attempted during two August evenings in 1996 experienced high water vapor turbulence in the atmosphere, and phase referencing was not successful.) The observing frequency was 43.2 GHz and we observed four 8 MHz bands, each at right and left circular polarization. We employed 2-bit sampling at the Nyquist rate, which required the maximum aggregate sampling rate supported by the VLBA of 256 megabits per second. Only the inner five VLBA stations (Fort Davis, Los Alamos, Pie Town, Kitt Peak, and Owens Valley) were used, as baselines longer than about 1500 km heavily resolve the scatter broadened image of Sgr A\* at 43 GHz (eg, Bower & Backer 1998).

The observing sequence involved rapid switching between compact extragalactic sources and Sgr A\*.

---

<sup>1</sup>The National Radio Astronomy Observatory is operated by Associated Universities Inc., under cooperative agreement with the National Science Foundation.

Two sources, J1745–283 and J1748–291, from the catalog of Zoonematkermani et al. (1990) were found to be strong enough ( $> 10$  mJy at 43 GHz) to serve as reference background sources. These sources are two of the three used by Backer & Sramek (1999) in their program to measure the proper motion of Sgr A\* with the VLA; their third background source, J1740–294, proved to have a steep spectrum and was too weak for inclusion in our 43 GHz program. We switched among the sources repeating the following pattern: Sgr A\*, J1745–283, Sgr A\*, J1748–291. Sources were changed every 15 seconds, typically achieving 7 seconds of on-source data, except for the earliest observation in 1995 when we were experimenting with longer switching times. We used Sgr A\* as the *phase-reference* source, because it is considerably stronger than the background sources and could be detected on individual baselines with signal-to-noise ratios typically between 10 and 20 in the 7 seconds of available on-source time.

We edited and calibrated data using standard tasks in the Astronomical Image Processing System (AIPS) designed for VLBA data. This involved applying data flagging tables generated by the on-line antenna and correlator systems, station gain curves, and system temperature measurements. We solved for station-dependent, intermediate-frequency band delays and phases on a strong, compact source (NRAO 530). After applying these corrections, the multi-band data for Sgr A\* could be combined coherently and interferometer phases as a function of time determined. These phase solutions were examined by an AIPS task specially written for our observations that looked for and flagged data when baseline-dependent phases on adjacent Sgr A\* scans changed by more than one radian. Under good weather conditions between 10 and 30% of the data were discarded by this process. This provided relatively unambiguous “phase connection” for the remaining data and allowed removal of most of the effects of short-term atmospheric fluctuations from all sources. (We note that during average-to-poor weather conditions, our phase measurements on Sgr A\* every 30 seconds were not frequent enough to provide unambiguous phase connection. Thus, our 15 second switching time is probably an optimum trade-off between on-source duty cycle and atmospheric coherence losses.) Data calibrated in this manner produced high (eg, 50:1) dynamic range maps of all sources with little or no spatial blurring. The images of the background sources appeared less resolved than that of Sgr A\*, with no signs of complex or multiple component structures.

We found that the differences in relative positions between a background source and Sgr A\* for closely spaced ( $\approx 10$  d) epochs were  $\approx 1$  mas. These differences exceeded the formal precision, estimated by the least-squares fitting process, typically by a large factor. Since the observational conditions and data analysis were nearly identical for these epochs, small geometric errors (eg, in baselines, source coordinates, or Earth’s orientation parameters) are unlikely to yield position shifts of this magnitude given the small angular separation of Sgr A\* and the background sources. Therefore, we evaluated the possibility that refractive scattering of the radio waves in the interstellar medium or modeling errors for the Earth’s atmospheric propagation delay could be responsible.

Refractive scattering can cause changes in the apparent flux density and position of a radio source. Gwinn et al. (1988) published VLBI observations that limit refractive position wander for water vapor masers in Sgr B2N, a star forming region close to the Galactic Center. For these maser spots, their 22 GHz observations revealed a diffractive scattering size of 0.3 mas and an upper limit to a Gaussian component of refractive position wander of 0.018 mas. Theoretical estimates of refractive position wander, based on the diffractive scattering size, by Romani, Narayan & Blandford (1986) agree with this limit for a Kolmogorov electron density spectrum. Assuming that the refractive effects scale as the diffractive scattering size, we expect any refractive wander of Sgr A\* at 43 GHz to be  $< 0.04$  mas, a value about a factor of 25 smaller than our observed position differences.

After careful study of the data, we concluded that the most likely source of relative position error is a small error in the atmospheric model used by the VLBA correlator. The following simple analysis supports this view: The phase-delay of the neutral atmosphere,  $\tau$ , can be approximated by  $\tau_0 \sec Z$ , where  $\tau_0$  is the vertical phase-delay and  $Z$  is the local source zenith angle. When measuring the *difference* in position of two sources separated in zenith angle by  $\Delta Z$ , a first-order Taylor expansion of  $\tau$  yields the expected *differenced* phase-delay error for a single antenna:

$$\Delta\tau \approx \frac{\partial\tau}{\partial Z} \Delta Z = \tau_0 \sec Z \tan Z \Delta Z . \quad (1)$$

The seasonally-averaged atmospheric model (Niell 1996) used by the VLBA correlator is likely to miss-estimate  $\tau_0$  by about 0.1 nsec, equivalent to a zenith phase-delay of  $\approx 3$  cm in path length. This comes mostly from the highly variable contribution by water vapor (eg, Treuhhaft & Lanyi 1987). Based on Eq. (1), this should result in an antenna-dependent error of  $\Delta\tau \approx 0.3$  cm for typical source zenith angles of  $\approx 70^\circ$  and for our typical source separations of  $\Delta Z \approx 0.012$  rad ( $\approx 0.7^\circ$ ). Since atmospheric errors are largely uncorrelated for different antennas, on an interferometer baseline at an observing wavelength of 0.7 cm, we would expect a relative position shift of roughly  $\sqrt{2} \times 0.3$  cm or  $\approx 70\%$  of a fringe spacing. This corresponds to  $\approx 0.4$  and  $\approx 1.7$  mas in the easterly and northerly directions, respectively, for our longer baselines. This effect should only partially cancel among the different baselines and can explain the position errors seen in the raw maps made from observations made  $\approx 10$  days apart.

In order to improve our relative position measurements, we modeled simultaneously our differenced-phase data for the “J1745–283 minus Sgr A\*” and “J1748–291 minus Sgr A\*” source pairs. The model allowed for a relative position shift for each source pair and a single vertical atmospheric delay error in the correlator model for each antenna. This approach significantly improved the accuracy of the relative position measurements as evidenced by the smaller deviations in relative positions for observations closely spaced in time. The vertical atmospheric delay parameters typically indicated a correlator model error of a few cm and these parameters were estimated with uncertainties of about 1 cm. Using this approach, we would estimate from Eq. (1) and the above discussion that relative position errors should be  $\approx 0.1$  and  $\approx 0.4$  mas in the East–West and North–South coordinates, respectively, for one day’s observation.

The differenced-phases often displayed post-fit residuals of  $\sim 30$  degrees of phase, which were correlated over periods of hours. Assuming equal and uncorrelated contributions from the two antennas forming an interferometer pair, this suggests a delay change of about 0.1 nsec of time or about 3 cm of uncompensated path length. Since typical source zenith angles were about 70 degrees, this corresponds to a vertical delay change in the atmosphere above each antenna of about 0.03 nsec or about 1 cm of path length. This behavior is consistent with expected large-scale changes in the atmospheric delay, and it suggests that significant improvement can be obtained by monitoring and correcting for large scale atmospheric changes.

The data in Table 1 summarize our relative position measurements. The data taken on 1995 March 4 were of poor quality, only the stronger of the two background sources (J1745–283) was detected, and the positional accuracy was significantly worse than for the later epochs. Positions of the strongest background source, J1745–283, phase-referenced to Sgr A\*, for epochs spanning 2 years are plotted in Fig. 1 with open circles in the sense Sgr A\* relative to J1745–283. They indicate a clear apparent motion for Sgr A\* relative to J1745–283, consistent in magnitude and direction with the reflex motion of the Sun around the Galactic Center (see §3.1). The positions in the East–West direction have typical uncertainties of about 0.1 mas, as estimated from the scatter of the post-fit position residuals about a straight-line motion. It is interesting to note that, while it takes  $\approx 220$  My for the Sun to complete an orbit around the Galactic Center, the East–West component of the parallax from only 10 days motion can be detected with the VLBA! The

position uncertainties in the North-South direction are larger, about 0.4 mas, owing to the low declination of the Galactic Center.

The apparent motions of Sgr A\* relative to J1745–283 over a 2 year time period and J1748–291 relative to J1745–283 over a 1 year time period are given in Table 2. The uncertainties in Table 2 include estimates of the systematic effects, dominated by errors in modeling of atmospheric effects, as discussed above. Assuming that J1745–283 is sufficiently distant that it has negligible intrinsic angular motion, Sgr A\*’s apparent motion is  $-3.33 \pm 0.1$  and  $-4.94 \pm 0.4$  mas  $y^{-1}$  in the easterly and northerly directions, respectively. This motion is shown by the solid lines in Fig. 1.

As a check on the accuracy of our measurements, we measured relative positions between the two calibration sources. These positions are plotted in Fig. 1 (crosses) in the sense “J1748–291 minus J1745–283,” offset to fit the plotting scale for the “Sgr A\* minus J1745–283” data. The best fit motions are  $+0.17 \pm 0.14$  and  $-0.22 \pm 0.56$  mas  $y^{-1}$  in the easterly and northerly directions, respectively, as indicated with the dashed lines in Fig. 1. The *uncertainty* in the relative motion of J1748–291 with respect to J1745–283 is  $\approx 40\%$  larger than for the motion of Sgr A\* with respect to J1745–283, because the angular separation of the two background sources ( $\approx 1.0$  deg) is greater than between Sgr A\* and either of the background sources ( $\approx 0.7$  deg). Thus, the background sources display no statistically significant motion relative to each other, as expected for extragalactic sources.

Finally, we have determined the position of Sgr A\* relative to an extragalactic source with high accuracy and, therefore, can derive an improved absolute position of Sgr A\*. VLBI observations carried out by the joint NASA/USNO/NRAO geodetic/astrometric array (Eubanks, private communication) detected J1745–283 at 8.4 GHz and determined its position in the U.S. Navy 1997-1998 reference frame to be

$$\text{J1745–283} \quad \alpha(2000)=17 45 52.4968, \quad \delta(2000)=-28 20 26.294,$$

with a uncertainty of about 12 mas. Assuming this result, we find the position of Sgr A\* measured at 1996.25 to be

$$\text{Sgr A*} \quad \alpha(2000)=17 45 40.0409, \quad \delta(2000)=-29 00 28.118.$$

The uncertainty in this position is dominated by that of J1745–283. Note that were one not to correct for the “large” apparent proper motion of Sgr A\*, the position of Sgr A\* determined for observations made more than 2 years from 1996.25 would be shifted by an amount greater than the  $\approx 12$  mas uncertainty.

### 3. Discussion

The apparent motion of Sgr A\* with respect to background radio sources can be used to estimate the rotation of the Galaxy and any peculiar motion of the super-massive black hole candidate Sgr A\*. In Fig. 2 we plot the change in apparent position on the plane of the sky of Sgr A\* relative to J1745–283. The dotted line is the variance-weighted least-squares fit to the data, and the solid line denotes the orientation of the Galactic Plane. Clearly the apparent motion of Sgr A\* is almost entirely in the Galactic Plane. Thus, it is natural to convert the apparent motion from equatorial to galactic coordinates. For Sgr A\* relative to J1745–283, this yields an apparent motion of  $-5.90 \pm 0.35$  and  $+0.20 \pm 0.30$  mas  $y^{-1}$  in galactic longitude and latitude, respectively. The apparent motion in the plane of the Galaxy should be dominated by the effects of the orbit of the Sun around the Galactic Center, while the motion out of the plane should contain only small terms from the Z-component of the Solar Motion and a possible motion of Sgr A\*. In the following subsections, we investigate the various components of the apparent motion of Sgr A\*, place limits on any offset of Sgr A\* from the dynamical center of the Galaxy, derive limits on the mass of Sgr A\*, and

constrain the distribution of dark matter in the Galactic Center.

### 3.1. Motion of Sgr A\* in the Plane of the Galaxy

Assuming a distance of  $8.0 \pm 0.5$  kpc (Reid 1993), the apparent angular motion of Sgr A\* in the plane of the Galaxy translates to  $-223 \pm 19$  km s $^{-1}$ . The uncertainty includes the effects of measurement errors and the 0.5 kpc uncertainty in  $R_0$ . Provided that the peculiar motion of Sgr A\* is small (see §3.2), this corresponds to the reflex of true orbital motion of the Sun around the Galactic Center. This reflex motion can be parameterized as a combination of a circular orbit (i.e., of the LSR) and the deviation of the Sun from that circular orbit (the Solar Motion). The Solar Motion, determined from Hipparcos data by Dehnen & Binney (1998), is  $5.25 \pm 0.62$  km s $^{-1}$  in the direction of galactic rotation. Removing this component of the Solar Motion from the *reflex* of the apparent motion of Sgr A\* yields an estimate for  $\Theta_0$  of  $218 \pm 19$  km s $^{-1}$ . This value is consistent with most recent estimates of about 220 km s $^{-1}$  (Kerr & Lynden-Bell 1986) and can be scaled for different values of the distance to the Galactic Center by multiplying by  $R_0/8$  kpc.

The most straightforward comparison of our direct measurement of the *angular* rotation rate of the LSR at the Sun ( $\Theta_0 / R_0$ ) can be made with Hipparcos measurements based on motions of Cepheids. Feast & Whitelock (1997) conclude that the angular velocity of circular rotation at the Sun,  $\Theta_0 / R_0$  (= Oort's A–B), is  $27.19 \pm 0.87$  km s $^{-1}$  kpc $^{-1}$  ( $218 \pm 7$  km s $^{-1}$  for  $R_0 = 8.0$  kpc). Our value of  $\Theta_0 / R_0$ , obtained by removing the Solar Motion in longitude from the *reflex* of the motion of Sgr A\* in longitude, is  $27.2 \pm 1.7$  km s $^{-1}$  kpc $^{-1}$ . The VLBA and Hipparcos measurements are consistent within their joint errors, and both measurements are insensitive to the value of  $R_0$ , as it is only used to remove the small contribution of the Solar Motion. It is important to note that our value of  $\Theta_0 / R_0$  is a true “global” measure of the angular rotation rate of the Galaxy. The consistency of the local (A–B) and global measures of  $\Theta_0 / R_0$  suggests that local variations in Galactic dynamics ( $d\Theta_0 / dR_0$ ) are less than the joint uncertainties of about 2 km s $^{-1}$  kpc $^{-1}$ .

After removing the best estimate of the motion of the Sun around the Galactic Center, our VLBA observations yield an estimate of the peculiar motion of Sgr A\* of  $0.0 \pm \sqrt{0.87^2 + 1.7^2}$  km s $^{-1}$  kpc $^{-1}$  or  $0 \pm 15$  km s $^{-1}$  towards positive galactic longitude. This estimate of the “in plane” motion of Sgr A\* comes from differencing two *angular* motions. Since this difference is negligible, the uncertainty in  $R_0$  does not affect this component of the peculiar motion of Sgr A\*. Given the excellent agreement in the global and local measures of the angular rotation rate of the Galaxy, and the lack of a detected peculiar motion for Sgr A\*, it is likely that Sgr A\* is at the dynamical center of the Galaxy.

### 3.2. Motion of Sgr A\* out of the Plane of the Galaxy

Whereas the orbital motion of the Sun (around the Galactic Center) complicates estimates of the “in plane” component of the peculiar motion of Sgr A\*, motions out of the plane are simpler to interpret. One needs only to subtract the small Z-component of the Solar Motion from the observed motion of Sgr A\* to estimate the out-of-plane component of the peculiar motion of Sgr A\*. An implicit assumption in this procedure is that the Solar Motion reflects the true peculiar motion of the Sun. Since most estimates of the Solar Motion are relative to stars in the solar neighborhood, this assumes that “local” and “global” estimates of the Solar Motion are similar. This procedure could be compromised slightly were the solar neighborhood to have a significant motion out of the plane of the Galaxy, owing, for example, to a galactic

bending or corrugation mode.

One way to limit the magnitude of a possible difference between a local and global estimate for the Solar Motion is to compare motions based on nearby stars with those based on much more distant stars. Using stars within about 0.1 kpc Dehnen & Binney (1998) find the Z-component for the Solar Motion to be  $7.17 \pm 0.38 \text{ km s}^{-1}$ , while Feast & Whitelock (1997) determine a value of  $7.61 \pm 0.64 \text{ km s}^{-1}$  for stars with distances out to a few kpc. Since these values agree within their joint uncertainties of about  $0.74 \text{ km s}^{-1}$ , it seems unlikely that local and global values for the Solar Motion could differ by more than about  $1 \text{ km s}^{-1}$ .

The Hipparcos measurements of large numbers of stars in the solar neighborhood provide an excellent reference for determining the local solar motion. We adopt the value of Dehnen & Binney (1988), which comes from the velocities of more than 10,000 stars within about 0.1 kpc of the Sun. Removing  $7.17 \text{ km s}^{-1}$  from our measured apparent motion of Sgr A\* out of the plane of the Galaxy, we estimate the peculiar motion of Sgr A\* to be  $15 \pm 11 \text{ km s}^{-1}$  toward the north galactic pole (see Table 3). The uncertainty is dominated by our proper motion measurements and can be greatly improved by future measurements. Note, for example, that increasing the weight (decreasing the estimated uncertainty) of the 1995 measurement would decrease the magnitude of our peculiar motion estimate. We do not consider our estimate of the peculiar motion of Sgr A\* out of the plane of the Galaxy to be statistically distinguishable from a null result.

### 3.3. Limits on the Mass of Sgr A\*

Our estimates of a peculiar motion of Sgr A\* provide an upper limit of about  $20 \text{ km s}^{-1}$  each for motions in and out of the galactic plane. Since stars in the inner-most regions of the central cluster move at speeds in excess of  $1000 \text{ km s}^{-1}$  (Eckart & Genzel 1997, Ghez et al. 1999), a central “dark mass” of approximately  $2.6 \times 10^6 M_\odot$  contained within 0.015 pc of Sgr A\* seems required. It is likely, but unproven, that most of this mass is contained in a super-massive black hole: Sgr A\*. Given the fact that independent measurements (Backer & Sramek 1999, and this paper) show that Sgr A\* moves at least two orders of magnitude slower than its surrounding stars, Sgr A\* must be much more massive than the  $\sim 10 M_\odot$  stars observed in the central cluster. (See also Gould & Ramírez [1998] for discussion of the implications of a lack of apparent *acceleration* of Sgr A\*.) In this section we derive a lower limit to the mass of Sgr A\* and constrain possible distributions of dark matter, not in the form of a super-massive black hole.

#### 3.3.1. Virial Theorem

Unfortunately, the Virial theorem is of little help in relating the masses and velocities of stars to that of a central massive black hole. For Virial equilibrium,

$$T_s + T_{bh} = -\frac{1}{2} (U_s + U_{bh}) \quad , \quad (2)$$

where  $T$  and  $U$  correspond to the kinetic and potential energy terms and the subscripts  $s$  and  $bh$  identify those associated with the stars and a central, massive, black hole, respectively. Essentially all the kinetic energy can be tied up in the stars ( $T_s$ ) and all the gravitational potential energy found associated with the black hole ( $U_{bh}$ ). In this case, attempts to estimate the kinetic energy of the black hole ( $T_{bh}$ ) require differencing two large and uncertain quantities and will be essentially useless.

### 3.3.2. Equipartition of Kinetic Energy

Upper limits on the motion of Sgr A\* have been used to infer lower limits on the mass of Sgr A\* by assuming equipartition of kinetic energy (eg, Backer 1996, Genzel et al. 1997). This is reasonable for stellar systems such as globular clusters, where massive stars are found concentrated toward the cluster center and move more slowly than lower mass stars. Similar results might also hold for a system involving a central black hole and a surrounding stellar cluster, provided the core mass of the cluster *greatly exceeds* that of the black hole. However, given the likely mass dominance of Sgr A\* over the stars within 0.015 pc, where high stellar speeds have been measured, equipartition of kinetic energy may be an unreliable approximation.

Indeed, our solar system may prove a better “scale model” (with planets corresponding to stars and the Sun corresponding to Sgr A\*). The Sun orbits the barycenter of the solar system, approximately in a binary orbit with Jupiter. Neglecting small perturbations from other planets, for a binary orbit in the center of mass frame, momentum conservation requires that  $m_J v_J = M_\odot V_\odot$ , where the subscripts  $J$  and  $\odot$  refer to Jupiter and the Sun, respectively. The ratio of the kinetic energy of Jupiter to the Sun is given by  $m_J v_J^2 / M_\odot V_\odot^2 = M_\odot / m_J$ . Hence, the kinetic energy of Jupiter exceeds that of the Sun by a factor equal to the inverse of the ratio of their masses and equipartition of kinetic energy does not apply.

### 3.3.3. Case 1: $M_{SgrA*} \sim 2.6 \times 10^6 M_\odot$

In order to better evaluate how an upper limit to the motion of Sgr A\* can be used to provide a lower limit to its mass, we carried out N-body simulations of stars orbiting about a massive black hole. We used a simple, direct integration code (NBODY0) of Aarseth (1985), documented by Binney & Tremaine (1987) and modified for our purposes. Initial simulations used 255 stars orbiting a  $2.6 \times 10^6 M_\odot$  black hole. The stellar masses were chosen randomly to represent the upper end of a stellar mass function with a power law distribution from 20 down to  $2 M_\odot$ . The number of stars and their masses used in this simulation are comparable to those observed within the central 0.5 arcsec, or 4000 AU (Genzel et al. 1997). Stellar orbits were chosen by randomly assigning a distance from the black hole, uniformly distributed in the range 10 to 10,000 AU, calculating a circular orbital speed, and then adjusting the speed randomly by between  $\pm 20\%$  of the circular speed for each of the three Cartesian coordinates. Before starting the N-body integrations, the orbital orientations were randomized by rotating the coordinates (and velocity components) through three Euler rotations with angles chosen at random.

The N-body simulations show quasi-random motions of the massive black hole. After relatively short periods of time ( $\ll 10,000$  years) a “steady state” condition appeared to be reached. The speed of a typical star was about  $700 \text{ km s}^{-1}$  at an average distance of 6,000 AU. The motion of Sgr A\* changed completely in all three coordinates on time scales  $\ll 100$  years and was typically  $\lesssim 0.1 \text{ km s}^{-1}$  in each coordinate. The rapid, but bounded, changes in the motion of Sgr A\* suggests that close encounters with individual stars are responsible for most of the observed motions. Assuming this is the case, one can make a simple analytical estimate of the expected motion of Sgr A\*, owing to close encounters with stars in the dense central cluster.

For a two-body interaction conserving momentum and viewed in the center of mass frame,

$$mv = MV \quad , \quad (3)$$

where  $m$  and  $v$  are the mass and speed of the star and  $M$  and  $V$  are the mass and speed of the black hole, respectively. For the case of interest where  $M \gg m$ , the orbital speed of the star at periastron,  $v_p$ , is given

by the well known relation

$$v_p^2 = \frac{GM}{a} \left( \frac{1+e}{1-e} \right) , \quad (4)$$

where  $G$  is the gravitation constant,  $a$  is the stellar semi-major axis, and  $e$  is the orbital eccentricity.

Defining  $V_p$  as the speed of the black hole at periastron, combining Eqs. (3) and (4) yields

$$V_p = \left( \frac{m}{M} \right) \left( \frac{GM(1+e)}{a(1-e)} \right)^{1/2} . \quad (5)$$

Our observations are only sensitive to orbital periods longer than of order 1 year. Such orbital periods occur for stellar semimajor axes greater than about 50 AU (1000 Schwarzschild radii) for a  $2.6 \times 10^6 M_\odot$  black hole. Thus, for our application reasonable values for the parameters in Eq. (5) are as follows:  $m \sim 10 M_\odot$ ,  $e \sim 0.5$ , and  $a \sim 50$  AU, and the expected orbital speed of Sgr A\* would be  $\approx 0.03 \text{ km s}^{-1}$ . (We adopt the periastron speed, instead of the lower average orbital speed, because the influence of many orbiting stars will likely increase the speed of Sgr A\*, compared to the single star result.) This speed is well below our current limit for the motion of Sgr A\*. Thus, the simplest interpretation consistent with the fast stellar motions and the slow Sgr A\* motion is that Sgr A\* is a super-massive black hole.

### 3.3.4. Case 2: $M_{SgrA*} \ll 2.6 \times 10^6 M_\odot$

While the simplest interpretation is that Sgr A\* is a  $2.6 \times 10^6 M_\odot$  black hole, our upper limit on any peculiar motion for Sgr A\* currently is two to three orders of magnitude above its expected motion for that mass. Thus, it seems reasonable to investigate the possibility that the mass within a radius of 0.01 pc is not dominated by Sgr A\*, but instead is in some form of “dark” matter. In this case, Sgr A\* will react to the gravitational potential and orbit the center of mass of this dark matter. Below we show that the upper limits on the motion of Sgr A\* are complimentary to the stellar proper motion results and strongly constrain both the mass of Sgr A\* and any possible configuration of matter within the central 0.01 pc.

Fig. 3 displays the enclosed mass versus radius for four mass models that are consistent with the stellar proper motions (cf., Genzel et al. 1997, Ghez et al. 1999). These models all yield flat “enclosed-mass versus radius” relations at distances  $\gtrsim 0.01$  pc from the center of mass of the system where measurements exist. The most centrally condensed mass distribution, a point mass, is shown as the horizontal dash-dot line labeled “a”. The least centrally condensed mass distribution plotted is for a Plummer density distribution, where density,  $\rho$ , is given by  $\rho = \rho_0 (1 + (r/r_0)^2)^{-\alpha/2}$ , for  $\rho_0 = 6 \times 10^{11} M_\odot \text{ pc}^{-3}$ ,  $r_0 = 0.01$  pc, and  $\alpha = 5$ . This distribution is shown with a curved dash-dot line labeled “d”. It is difficult to make a physically reasonable mass distribution that is significantly less centrally condensed than this and consistent with the stellar motion data. These two “extreme” model distributions approximately bound all allowed mass distributions; two particular examples of intermediate models are shown in Fig. 3 with dashed curves labeled “b” and “c”.

Assuming that Sgr A\* has a mass  $\ll 10^6 M_\odot$ , it will orbit about the center of mass of the system. Orbital speed for a body at a radius,  $r$ , from the center of mass is given by  $V = \sqrt{GM_{encl}/r}$ , where  $M_{encl}$  is the enclosed mass at that radius. Setting  $V = 20 \text{ km s}^{-1}$ , our limit for the motion of Sgr A\*, produces the sloping solid line in Fig. 3. Only enclosed masses below that line are permitted by our observations. For radii greater than about  $3 \times 10^{-5}$  pc (6 AU), this limit rules out all but the *least* centrally condensed mass models. For radii less than about  $3 \times 10^{-5}$  pc, the orbital motion of Sgr A\* produces angular excursions less than 0.8 mas. In this case, while the orbital speed might greatly exceed  $20 \text{ km s}^{-1}$ , we may have failed

to detect these excursions owing to our poor temporal sampling and  $\approx 0.4$  mas errors in the North–South direction. Thus, we do not extend the motion limit line below  $3 \times 10^{-5}$  pc, and at this radius we replace the motion limit with a vertical line in Fig. 3.

The stellar proper motions and the limits on the proper motion of Sgr A\* combine to exclude almost all of “parameter space” for models of the density distribution of material in the inner 0.1 pc of the Galactic Center. The stellar motions exclude “soft” gravitational potentials (i.e., the least centrally condensed mass distributions) and the motion limit for Sgr A\* excludes “hard” gravitational potentials. Continued VLBA observations of Sgr A\* over the next five years could reduce the uncertainty in the peculiar motion of Sgr A\* to about  $2 \text{ km s}^{-1}$  (dotted line in Fig. 3) out of the plane of the Galaxy. Improved accuracy for positions in individual VLBA observations, necessary for a trigonometric parallax of Sgr A\*, could move the small angular excursion limit to  $< 0.2$  mas. This would further and drastically restrict the range of possible models for a dominant central dark matter condensation.

The point-like mass distribution labeled “a” in Fig. 3 essentially requires a super-massive black hole. Since we have assumed in this section that this is **not** Sgr A\*, we would be left with the question of why a low-mass Sgr A\* radiates far more than a super-massive black hole in essentially the same environment. Other mass models, and especially those with the most centrally condensed mass distributions (eg, labeled “b” in Fig. 3) require exceedingly high mass densities. For example, model “b” has  $\approx 5 \times 10^5 M_\odot$  within a radius of 6 AU, resulting in a density of  $10^{19} M_\odot \text{ pc}^{-3}$ . Theoretical arguments suggest that such models are unlikely to be stable for even  $10^7$  y, regardless of the composition of the matter (Maoz 1998).

The hardest cases to exclude on either observational or theoretical grounds are given by the mass distributions that are the least centrally condensed, but still consistent with the stellar motion data. For this case, one can ask the question, at what mass will perturbations by stars in the central cluster lead to detectable motion of Sgr A\*? In order to answer this question, we modified the N-body code described in § 3.3.3 to include a fixed gravitational potential appropriate for a Plummer law mass distribution with  $\alpha = 5$ ,  $\rho_0 = 6 \times 10^{11} M_\odot \text{ pc}^{-3}$ , and  $r_0 = 0.01$  pc (model “d”). Sgr A\* was assigned a mass ( $\ll 10^6 M_\odot$ ) and the entire system, including 254 stars was allowed to evolve in time. For the softer allowable gravitational potentials (eg, “c” and “d”) there is little enclosed mass within  $\sim 10^{-4}$  pc to bind Sgr A\*. We found that when Sgr A\*’s mass was less than  $\approx 3,000 M_\odot$ , Sgr A\* gradually moved outward from the center of the gravitational potential and achieved orbital speeds in excess of  $20 \text{ km s}^{-1}$ . Thus, we conclude that the lack of detectable motion for Sgr A\* places a conservative lower limit of about  $1,000 M_\odot$  for the mass associated with Sgr A\*.

#### 4. Conclusions

The *apparent* proper motion of Sgr A\*, relative to extragalactic sources, is consistent with that expected from the Sun orbiting the center of the Galaxy. Thus, Sgr A\* must be very close to, and most likely at, the dynamical center of the Galaxy. In this case, the proper motion measurement gives the angular rotation speed at the Sun,  $(\Theta_0 + V_\odot)/R_0$ , directly, from which we estimate  $\Theta_0 = 218 \pm 19 \text{ km s}^{-1}$  for  $R_0 = 8 \text{ kpc}$ .

Our lower limit for the peculiar motion of Sgr A\* of about  $20 \text{ km s}^{-1}$  implies a lower limit for mass of Sgr A\* of  $\sim 10^3 M_\odot$ . This rules out the possibility that Sgr A\* is any known multiple star system, such as a contact binary containing  $\sim 10 M_\odot$  and radiating near its Eddington luminosity. A mass of more than  $\sim 10^3 M_\odot$  and a luminosity  $\lesssim 10^5 L_\odot$  indicates that Sgr A\* is radiating at  $\lesssim 0.1\%$  of its Eddington limit.

All observations are consistent with Sgr A\* being a super-massive black hole. Since the lower limit for the mass of Sgr A\* is only about 0.1% of the gravitational mass inferred from the stellar motions, one cannot claim from our observations alone that even a significant fraction of the dark mass must be in Sgr A\*. However, alternative models involving “dark” matter distributions are severely restricted by observations.

Future VLBA observations should be able to reduce the uncertainty in the measurement of the motion of Sgr A\* out of the Galactic plane to  $\sim 0.2 \text{ km s}^{-1}$ , at which point knowledge of the Solar Motion may become the limiting factor. Should the peculiar motion of Sgr A\* be less than  $0.2 \text{ km s}^{-1}$ , then its mass almost certainly exceeds  $\sim 10^5 M_\odot$ . Such a large mass tied *directly* to the radio source, whose size is  $\lesssim 1 \text{ AU}$  from VLBI observations, would be compelling evidence that Sgr A\* is a super-massive black hole.

We thank D. Backer for providing coordinates for sources J1745–283 and J1748–291 early in our project, M. Eubanks for measuring the astrometric position of J1745–283, and V. Dhawan for helping with the VLBA setup.

## REFERENCES

Aarseth, S. 1985, in *Multiple Time Scales*, eds. J. U. Brackbill & B. I. Cohen, (Academic Press: New York), pp. 378–418

Backer, D. 1996, in *Unsolved Problems of the Milky Way*, eds. L. Blitz & P. Teuben, (Kluwer: Dordrecht), pp. 193–198

Backer, D. & Sramek, R.A. 1999, *this volume*

Balick, B. & Brown, R. 1974, ApJ, 194, 265

Binney, J. & Tremaine, S. 1987, *Galactic Dynamics*, (Princeton U. Press; Princeton)

Bower, G. C. & Backer, D. C. 1998, ApJ, 496, L97

Dehnen, W. & Binney, J. J. 1998, MNRAS, 298, 387

Eckart, A. & Genzel, R. 1997, MNRAS, 284, 576

Feast, M. & Whitelock, P. 1997, MNRAS, 291, 683

Genzel, R., Eckart, A. Ott, T. & Eisenhauer, F. 1997, MNRAS, 291, 219

Ghez, A. M., Klein, B. L., Morris, M. & Becklin, E. E. 1999, to appear in ApJ

Gould, A. & Ramírez, S. V. 1998, ApJ, 497, 713

Gwinn, C. R., Moran, J. M., Reid, M. J. & Schneps, M. H. 1988, ApJ, 330, 817

Kerr, F. J. & Lynden-Bell, D. 1986, MNRAS, 221, 1023

Maoz, E. 1998, ApJ, 494, L181

Menten, K. M., Reid, M. J., Eckart, A. & Genzel, R. 1997, ApJ, 475, L111

Niell, A. E. 1996, JGR, 101, 3227

Reid, M. J. 1993, ARA&A, 31, 345

Romani, R. W., Narayan, R. & Blandford, R. 1986, MNRAS, 220, 19

Serabyn, E., Carlstrom, J., Lay, O., Lis, D. C., Hunter, T. R., Lacy, J. H. & Hills, R. E. 1997, ApJ, 490, L77

Treuhaft, R. N. & Lanyi, G. E.. 1987, Rad. Sci., 22, 251.  
Zoonematkermani et al 1990, ApJS, 74, 181

Table 1. Residual Position Offsets Relative to Sgr A\*

Source	Date of Observation	East Offset <sup>a</sup> (mas)	North Offset <sup>a</sup> (mas)
J1745-283	1995 March 4	0.73	1.18
	1996 March 20	3.60	5.80
	1996 March 31	3.75	6.64
	1997 March 16	6.90	11.18
	1997 March 27	7.10	11.13
J1748-291	1996 March 20	27.55	82.07
	1996 March 31	27.53	81.98
	1997 March 16	31.00	86.92
	1997 March 27	31.09	86.60

<sup>a</sup>Uncertainties are 0.1 and 0.4 mas for the East and North offsets, respectively, for all epochs except 1995 March 4 which are estimated to be 0.5 and 0.8 mas owing to poor phase coherence.

Note. — Positions are relative to Sgr A\*, after removing the  $\approx 0.7$  degree differences. The origins are based on our originally adopted J2000 positions for Sgr A\* (17 45 40.0500, -29 00 28.120), J1745-283 (17 45 52.5056, -28 20 26.302), and J1748-291 (17 48 45.6930, -29 07 39.488).

Table 2. Apparent Relative Motions

Source – Reference		East Offset (mas y <sup>-1</sup> )	North Offset (mas y <sup>-1</sup> )	$\ell^{II}$ Offset (mas y <sup>-1</sup> )	$b^{II}$ Offset (mas y <sup>-1</sup> )
Sgr A*	– J1745–283	–3.33 (0.10)	–4.94 (0.40)	–5.90 (0.35)	+0.20 (0.30)
J1748–291	– J1745–283	+0.17 (0.14)	–0.22 (0.56)	–0.10 (0.56)	–0.26 (0.42)

Note. — Motions are based on data in Table 1, and estimated uncertainties are given in parentheses.

Table 3. Sgr A\*’s Motion in Galactic Coordinates<sup>a</sup>

Description	$\ell^{II}$ (km s <sup>-1</sup> )	$b^{II}$ (km s <sup>-1</sup> )
Observed Sgr A* motion	–223 (19)	8 (11)
Effects of Solar Motion <sup>b</sup> removed	–218 (19)	15 (11)
Effects of Galactic Rotation <sup>c</sup> removed	0 (15)	15 (11)

<sup>a</sup>Motions are for Sgr A\*, based on the J1745–283 (relative to Sgr A\*) data in Table 2. Speeds assume  $R_0 = 8.0 \pm 0.5$  kpc (Reid 1993). Quoted uncertainties given in parenthesis are 1- $\sigma$  and include measurement uncertainty and an angular-to-linear motion scaling error from the uncertainty in  $R_0$  .

<sup>b</sup>Adopted Solar Motion with respect to a circular orbit is  $5.25 \pm 0.62$  km s<sup>-1</sup> in  $\ell^{II}$  and  $7.17 \pm 0.38$  km s<sup>-1</sup> in  $b^{II}$  (Dehnen & Binney 1998).

<sup>c</sup>Adopted circular rotation of  $27.19 \pm 0.87$  km s<sup>-1</sup> kpc<sup>-1</sup> (Feast & Whitelock 1997) removed from our measured angular rotation rate of  $-27.2 \pm 1.9$  km s<sup>-1</sup> kpc<sup>-1</sup> (after correction for the Solar Motion) and then multiplied by  $R_0 = 8.0$  kpc. Since the angular motion difference is small, it is not sensitive to the value adopted for  $R_0$  when converting to linear motion. The quoted uncertainty is dominated by measurement uncertainties for the angular motions, scaled by  $R_0$  .

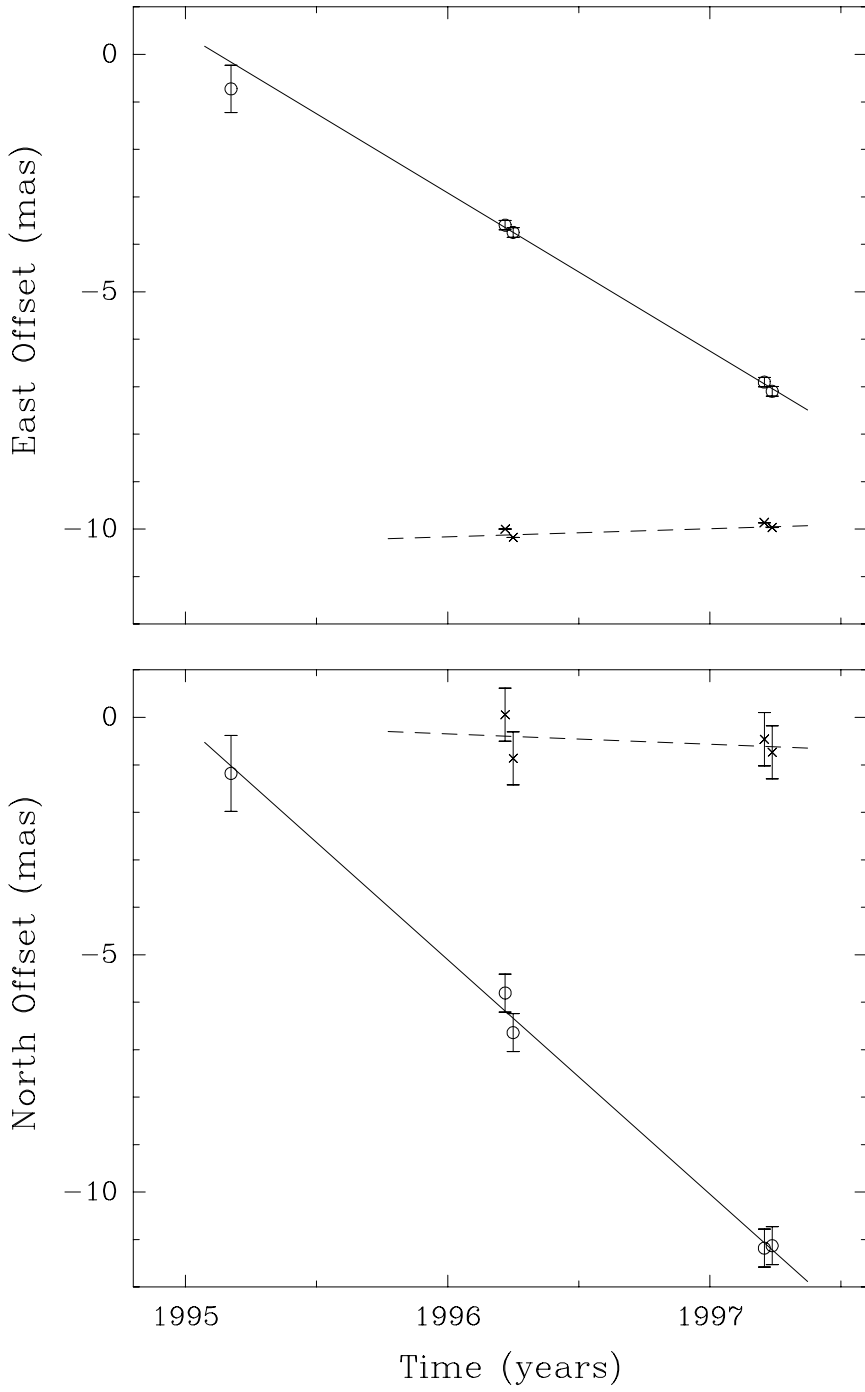


Fig. 1. Position residuals of Sgr A\* relative to J1745–283 (circles) and J1748–291 relative to J1745–283 (crosses) versus time. Eastward components are shown in the top panel and Northward components in the bottom panel. The solid and dashed lines give the variance-weighted best fit components of proper motion. The J1748–291–J1745–283 positions have been offset to fit the plot scale for the Sgr A\*–J1745–283 data.

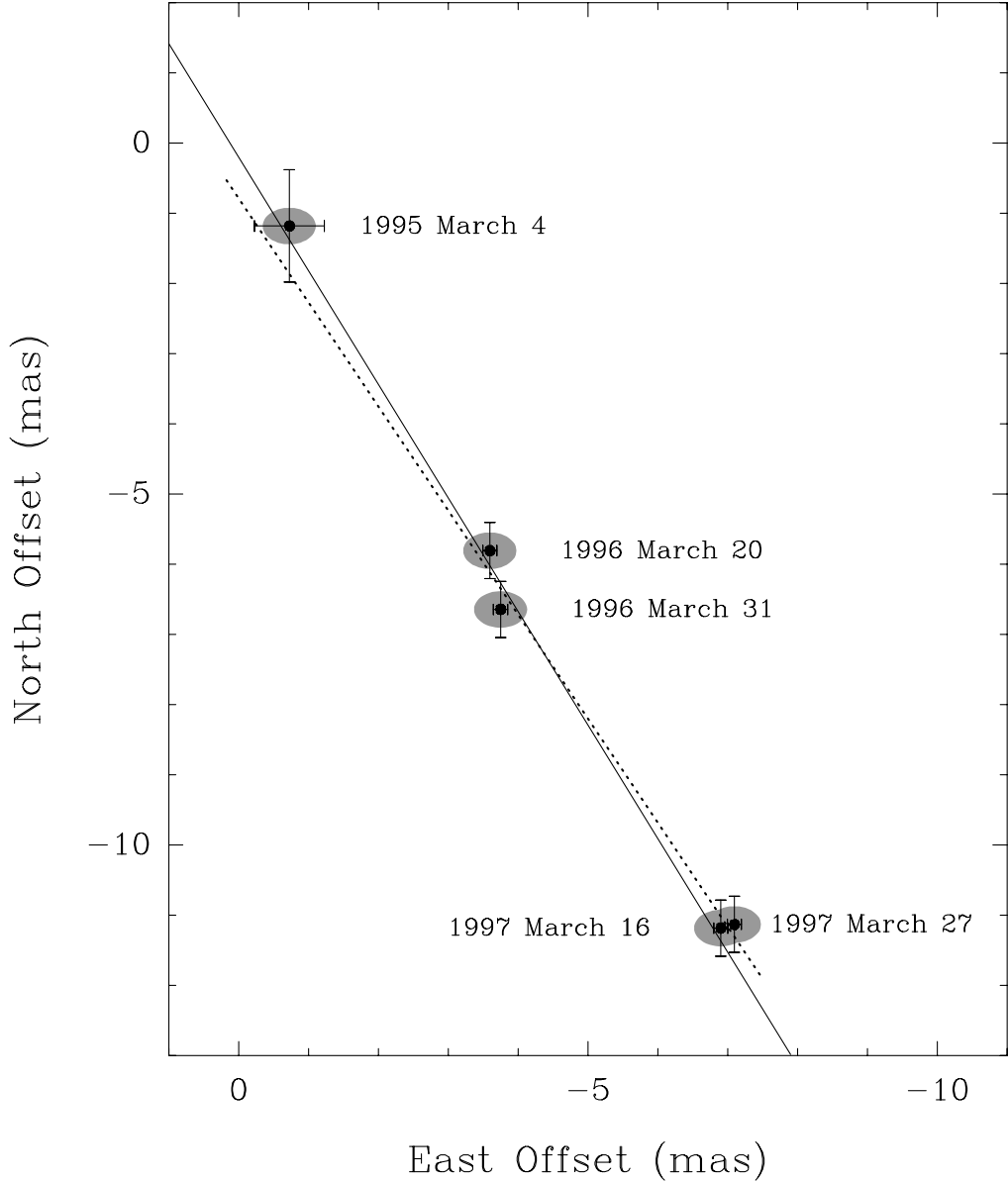


Fig. 2. Position residuals of Sgr A\* relative to J1745-283 on the plane of the sky. North is to the top and East to the left. Each measurement is indicated with an ellipse, approximating the apparent, scatter broadened size of Sgr A\* at 43 GHz, the date of observation, and  $1 - \sigma$  error bars. The dashed line is the variance-weighted best-fit proper motion, and the solid line gives the orientation of the Galactic plane.

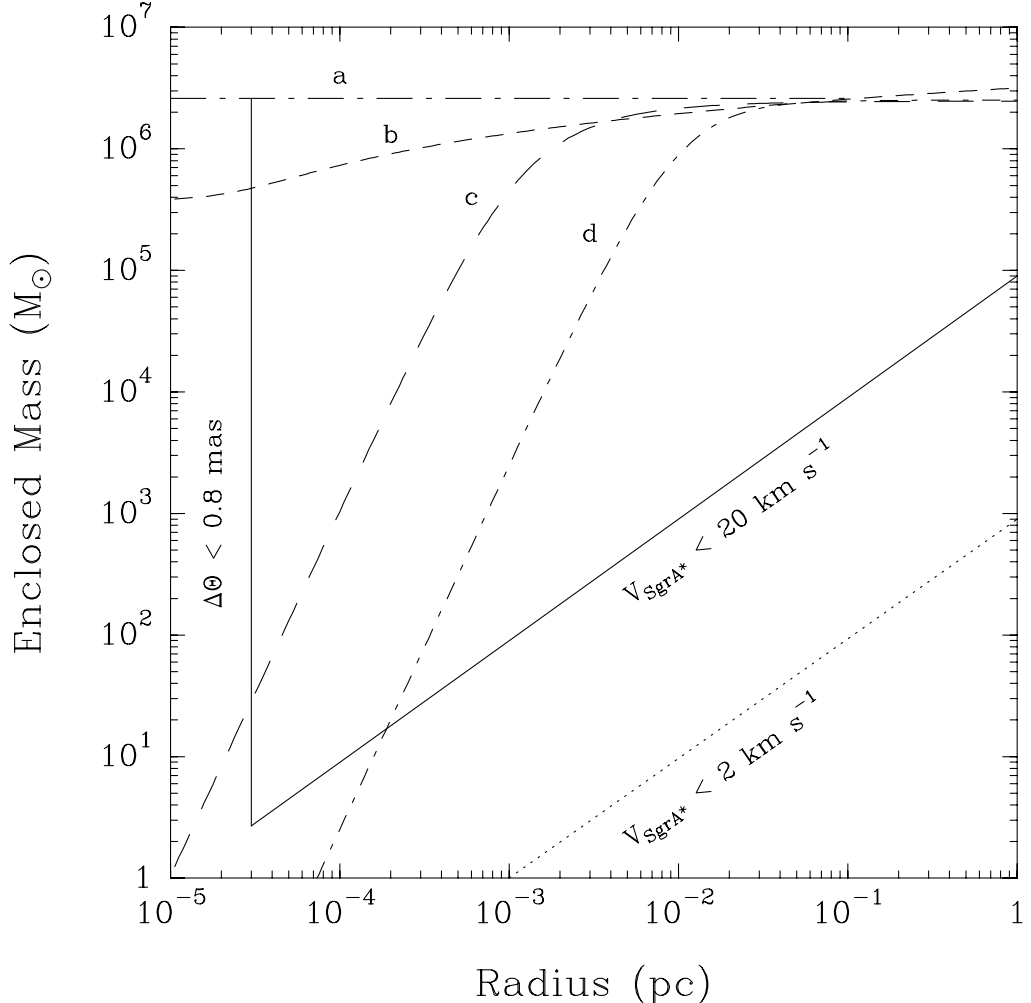


Fig. 3. Enclosed mass versus radius for various model distributions of dark matter, *assuming the mass of Sgr A\*  $\ll 10^6 M_\odot$* . Models labelled “a” through “d” have decreasing central mass condensations (progressively softer gravitational potentials) and approximately bound mass distributions that are consistent with stellar proper motion data. Model “a” is a point mass; model “b” through “d” have Plummer density distributions with  $\rho_0$  of  $3.9 \times 10^{18}$ ,  $2.5 \times 10^{14}$ , and  $6.0 \times 10^{11} M_\odot \text{ pc}^{-3}$ ;  $r_0$  of 0.00002, 0.001, and 0.01 pc; and  $\alpha$  of 3, 4, and 5, respectively. The sloping solid line indicates the upper limit for enclosed mass based on the proper motion of Sgr A\*. The vertical solid line at  $3 \times 10^{-5} \text{ pc}$  (6 AU) indicates the upper limit in radius, where angular excursions of Sgr A\* of  $< 0.8 \text{ mas}$  could be missed owing to insufficient astrometric accuracy. The sloping dotted line indicates expected improvement in the measurement of the proper motion of Sgr A\* within  $\approx 5$  years.